

Simulating Pellet and Clad Mechanical Interactions of Nuclear Fuel Rod for Pressure Water Reactors

W. Zhao, D. Mitchell, R. Oelrich

Westinghouse Electric Company LLC, Hopkins, SC29061 USA

Abstract

Pellet-cladding mechanical interaction (PCMI) is a potential failure mode leading to leaking fuel rods. Ever-increasing fuel duty and more demanding power maneuvers for adapting to alternative energy sources create new challenges for maintaining the high standard of fuel rod structural integrity. Towards meeting the new challenges, the paper describes an on-going effort in developing a coupled thermal-structural model suitable for simulating the complicated PCMI phenomena under normal operations, operational transients, and accident conditions. The models and various application examples are presented in the paper, including off-centered pellet, missing pellet surface, and pellet cracking. The work utilizes the commercial finite element software LS-DYNA® (LS-DYNA is a registered trademark by Livermore Software Technology Corporation, 7374 Las Positas Road, Livermore, CA 94550, www.lstc.com.)

1. Introduction

Fuel rods used in pressure water reactors (PWR) are made by enclosing enriched UO₂ pellets in thin walled Zirconium alloy cladding [1]. The fuel rod is built with an open pellet to clad gap that is reduced during operation due to a combination of irradiation and temperature driven cladding creep and fuel densification/swelling. Due to drastically different thermal and mechanical properties between these two components and large temperature gradients, excessive pellet-cladding mechanical interaction (PCMI) may occur during power increase, such as reactor startup following a refueling and return to power, where large tensile hoop stress at cladding inner surface due to pellet thermal expansion, assisted by corrosive fission products (such as iodine), causes cladding to crack and fail (leaking). Reference [2] provides a more complete description of failure mechanisms including irradiation and burnup related effects. PCMI can be exacerbated by pellet geometrical defects, e.g. a large missing pellet surface (MPS) that escaped inspections. Such an example is shown in Figure 1.

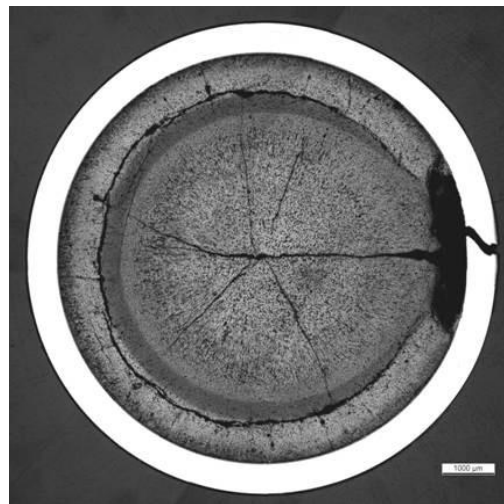


Figure 1 - Cross section of a failed fuel rod due to a large MPS.

As shown, a large MPS induced elevated hoop stress in clad and caused fuel rod failure, which was confirmed through Hotcell examinations [3]. Westinghouse has since greatly improved pellet inspection, implemented new reload evaluation method, and tighter power ramp limits based on comprehensive analyses [3]. Advanced core power monitoring system [4] is also in place to monitor each individual fuel rod in the core and evaluate the risk of PCMI failure in real time, providing guidance to reactor operators.

Although the PCMI-caused fuel rod failure in Westinghouse supplied fuel has become very rare (none observed since implementation of the improvements), development of more advanced simulation capability is necessary to better predict the behavior, further increase PCMI margin and operating flexibility, as well as to meet challenges from ever-increasing fuel duty and more demanding power maneuvers to adapt to needs of alternative energy sources. In addition, improved PCMI simulation capability allows for evaluation of technological solutions to increase PCI margin such as additive fuel. It is in this perspective that the paper describes an on-going effort in developing a coupled thermal-structural model suitable for simulating the complicated PCMI phenomena under steady-state operations, operational transients, and accident conditions, such as reactivity-induced accidents, or RIAs, where a power pulse occurs due to control rod ejection [5].

Localized failures caused by PCMI are a phenomenon dictated by power history, characteristics and behaviors of pellets and clad in a local region. Thus without losing generality, a section of a typical pressure water reactor (PWR) fuel rod is modeled in detail using LS-DYNA. The loading and boundary conditions for the LS-DYNA model are specified using fuel performance code [6], including pellet heat generation, rod internal gas mixture and pressure, gap conductance between pellet and clad, rod surface temperature and heat convection. Typical LS-DYNA models are described next, followed by examples and discussions.

2. Model Development

Over the course of the model development, different versions of the model were created with emphasis on different aspects of the PCMI phenomenon. Three representative models are described below. For reference, Figure 2(a) shows the geometry of a single pellet. It is a solid cylinder with dish and chamfer at each end. The diameter and height of the cylinder considered are about 8.2mm, and 9.8mm, respectively. Symmetry condition is used to model a section of the pellet and clad. Figure 2(b) is a model with 1/8 pellet used to consider fresh fuel with open gap and centered pellet. Three different materials are involved, ceramic UO₂ pellet, zirconium alloy clad, and the Helium gas (for fresh fuel, or gas mixture for burned fuel), which occupies the void formed by pellet chamfer and the clad. The gap between pellet and clad is represented using thermal and structural contact interface. The UO₂ pellet is modeled linear elastically with temperature dependent thermal and mechanical properties. The zirconium alloy clad has a multi-linear, temperature dependent, elastic-plastic stress strain curve, and a creep behavior represented by Garafalo's steady-state hyperbolic sine creep law (see LS-DYNA Keyword User's Manual Vol. 2, Material Models, *MAT_188, MAT_THERMO_ELASTO_VISCOPLASTIC_CREEP).

Likewise, Figure 3(a) is a model with 1/4 pellet used to consider fresh fuel with open gap and off-centered pellet. The generic load and boundary conditions are also shown in Figure 3(a). Figure 3(b) is a 1/8 model for two pellets used to consider fuel with closed gap. Models in Figure 2(b) and Figure 3(a) are used to consider two special cases where gap remains open throughout

the power ramp process. The model in Figure 3(b) (and a refined version seen later), with zero initial gaps, is used to study various PCMI cases in this paper.

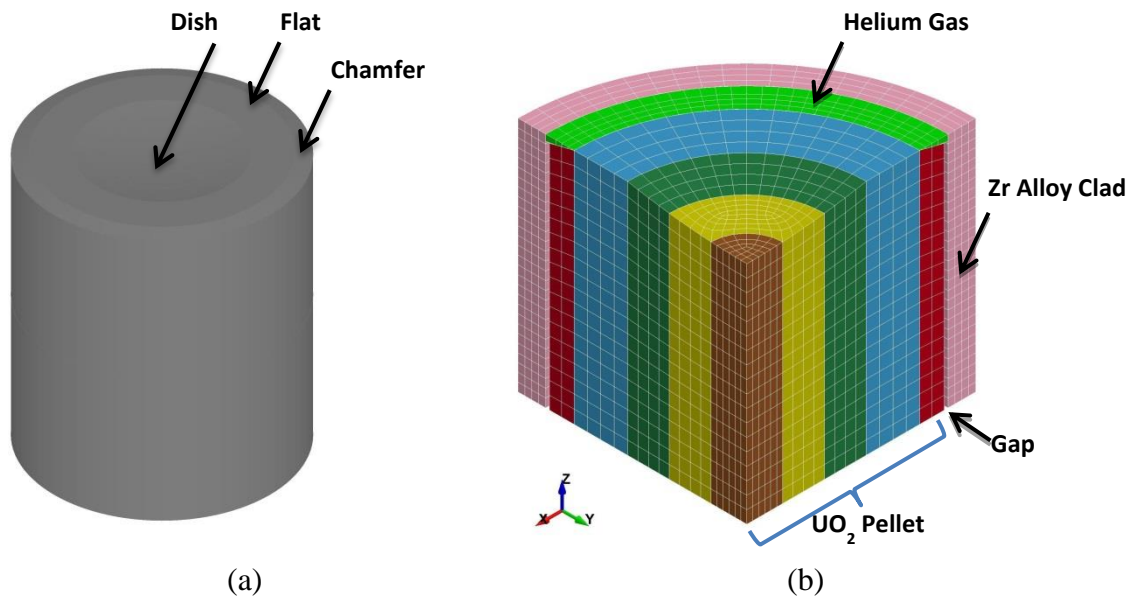


Figure 2 – (a) Geometry of a single pellet; (b) Model of 1/8 centered pellet and clad with open gap.

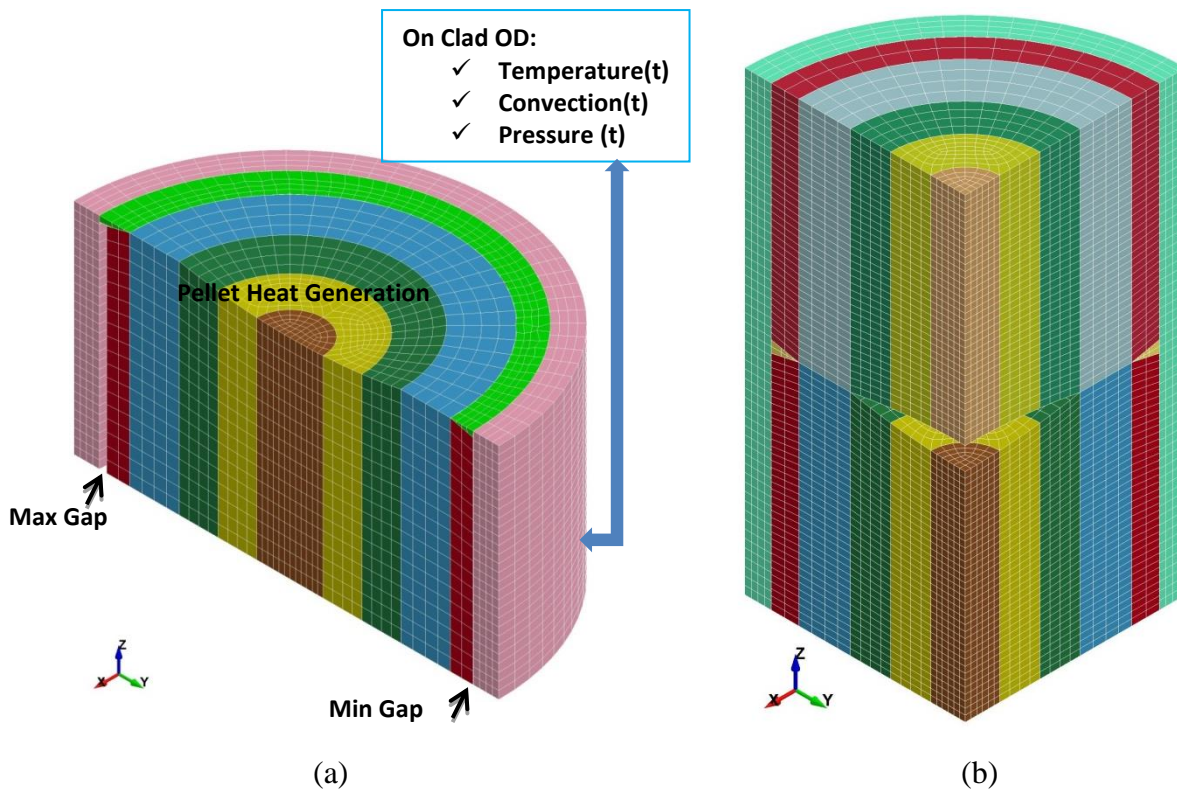


Figure 3 – (a) Model of 1/4 off-centered pellet and clad; (b) Model of 1/8 pellet and clad, zero initial gaps.

3. Examples and Discussions

Over the course of the model development, various examples of interest were considered to test the model, to study effects of various parameters on PCMI, and to gain more understanding of the PCMI behavior. Some of the examples are described in the following.

3.1 Open Gap with Centered Pellet

To start with, the simplest case of open gap with centered pellet was considered, whose model is shown in Figure 2(b). The gap size corresponds to the nominal gap for fresh fuel at room temperature. Since the gap remains open throughout the power ramp process, the pellet does not exert any forces on the clad; thus no cladding creep needs to be considered. Radiant heat transfer across the gap is also included, though not important at normal operating temperatures. The results for temperature contour at the end of a power ramp are shown in Figure 4.

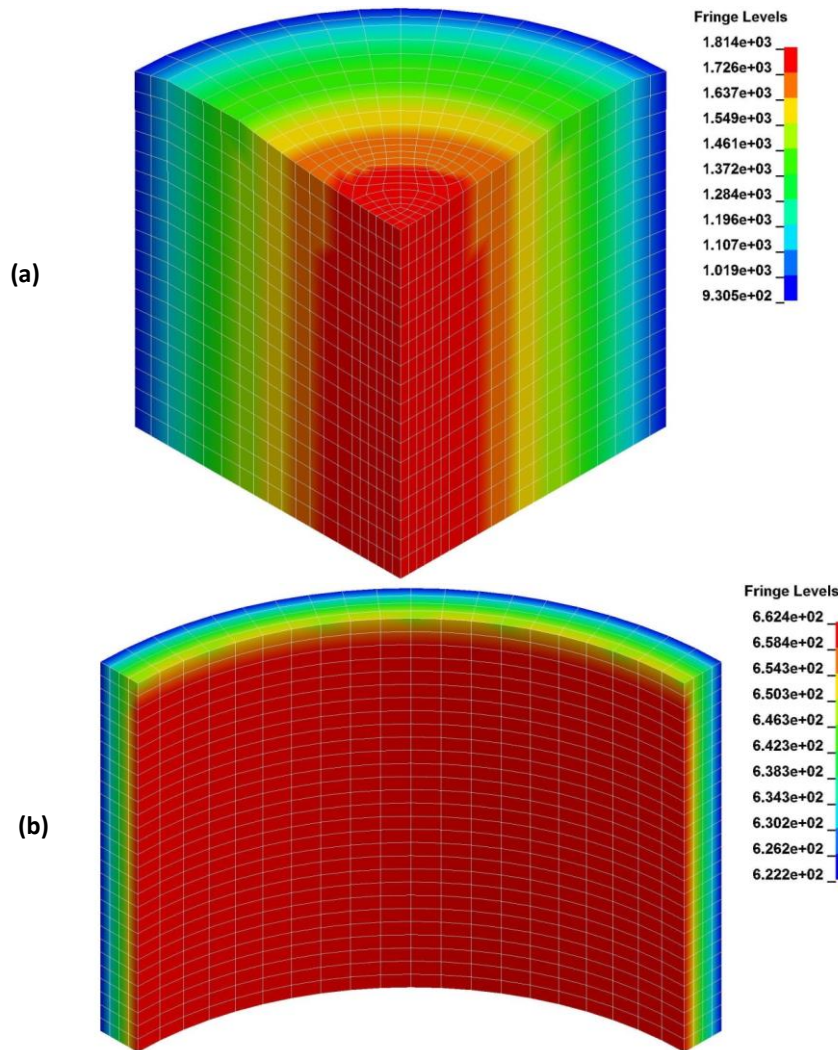


Figure 4: Temperature contour in Kelvin at the end of power ramp for (a) pellet; (b) clad.

The corresponding 1st principal stress contour and the vector field are shown in Figure 5. These results agree very well with expectations.

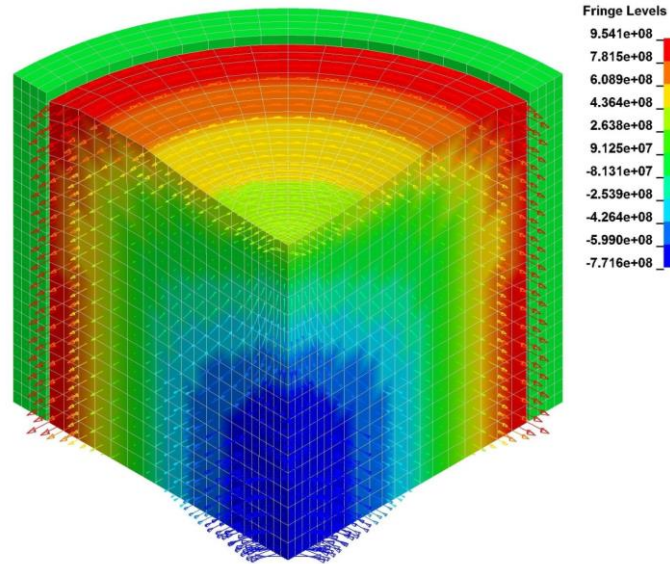


Figure 5: 1st principal stress contour and vector, Pa.

3.2 Open Gap with Off-Centered Pellet

Off-centered pellet is a most likely configuration for fresh fuel, and also provides an ideal case to examine the gap-dependent heat transfer behavior. As shown in Figure 3(a), the gap size increases from ~zero at the near side to the maximum at the far side, which is 165µm for the nominal dimension at room temperature.

The results for temperature contour at the end of the power ramp are shown in Figure 6(a) and (b). The temperature variation across the pellet diameter from min gap to the max gap is shown in Figure 7 at its top and bottom locations.

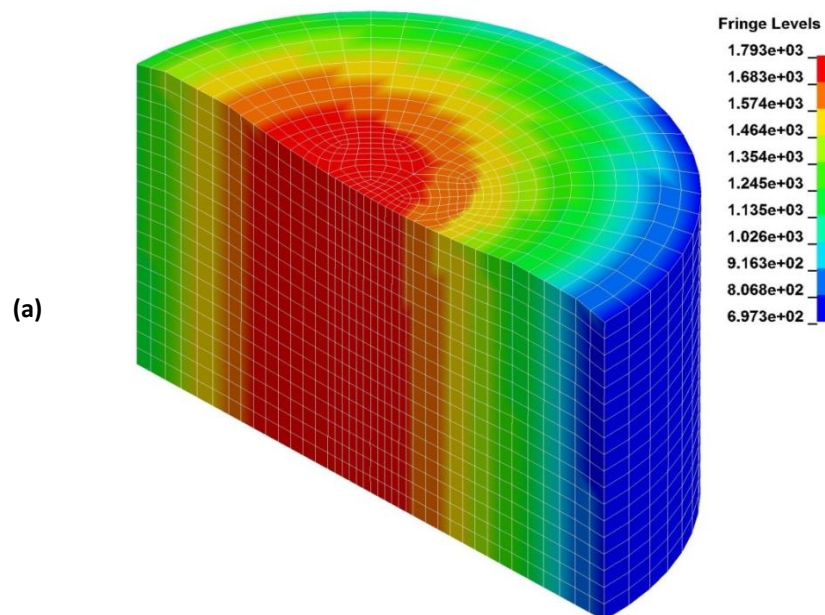


Figure 6(a): Temperature contour in Kelvin at the end of power ramp for pellet.

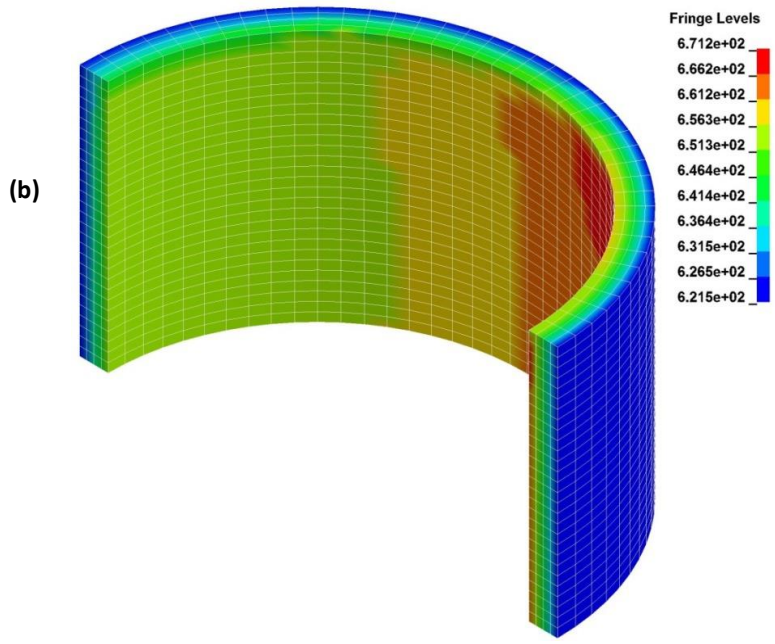


Figure 6(b): Temperature contour in Kelvin at the end of power ramp for clad.

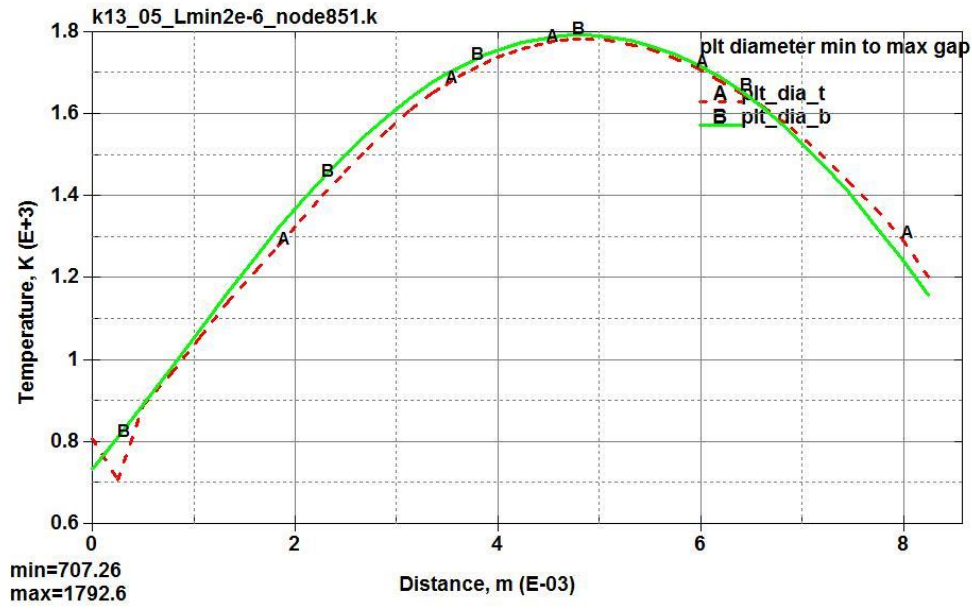


Figure 7: Pellet temperature variation across its diameter at the top and bottom locations.

These examples demonstrate an excellent capability of LS-DYNA in modeling detailed thermal-structural behaviors as occurred in PCMI.

3.3 Clad Ridging Effect

Due to pellet temperature gradients, both radially and axially, pellet deforms into an hour-glassed shape, causing clad to deform more radially at locations corresponding to pellet ends (chamfer edges). The

model shown in Figure 3(b) is used so that the power ramp starts at zero pellet-clad gaps. Symmetry boundary conditions are used on cut surfaces at bottom and sides. Different boundary conditions are considered at the top cut surfaces to assess its effect on ridging. The power ramp scheme used is shown in Figure 8, plus two variations of it: one with 600-hour additional hold time at the 50% power, the other with 1000-hour additional hold time at the 50% power. The creep law is active for all cases with closed gaps.

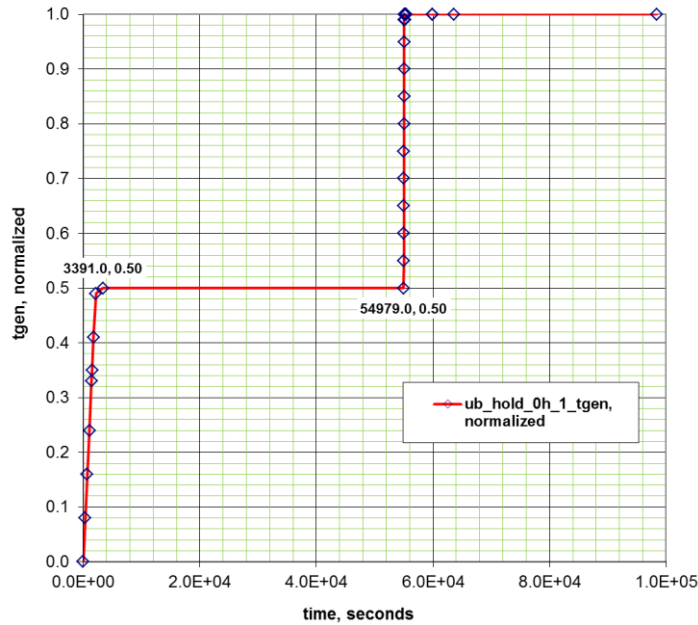


Figure 8: Power ramp scheme for 0 hour additional hold time (total time=27.3h).

The temperature contours at the end of the ramp are shown in Figure 9. The effective creep strain versus time at a few typical locations for the lower half of the clad is shown in Figure 10, with element locations identified: 6266 (ID) and 4586 (OD) at the mid height.

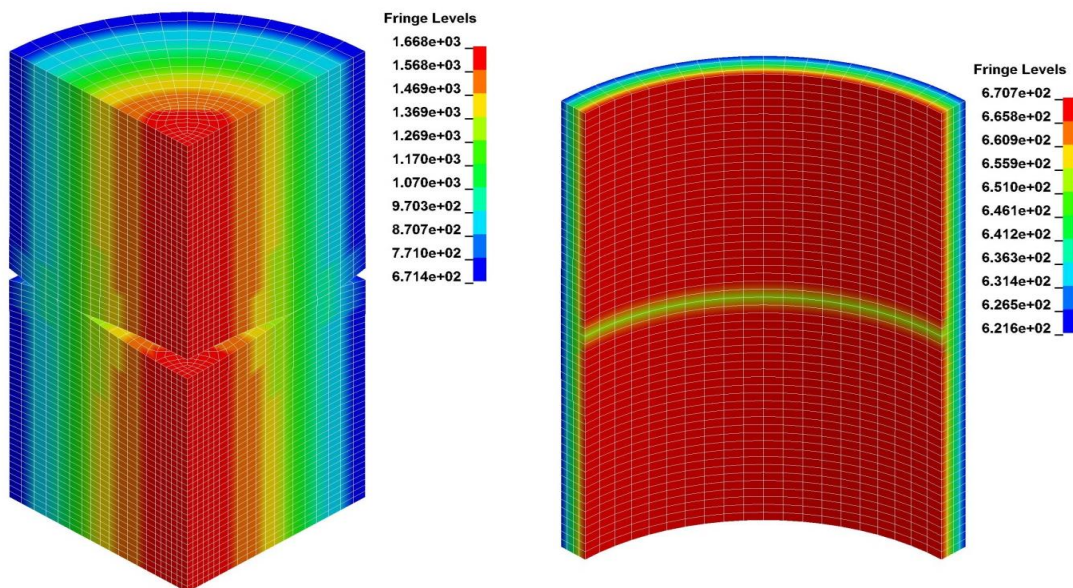


Figure 9: Temperature contours in K at the end of power ramp for pellet and clad.

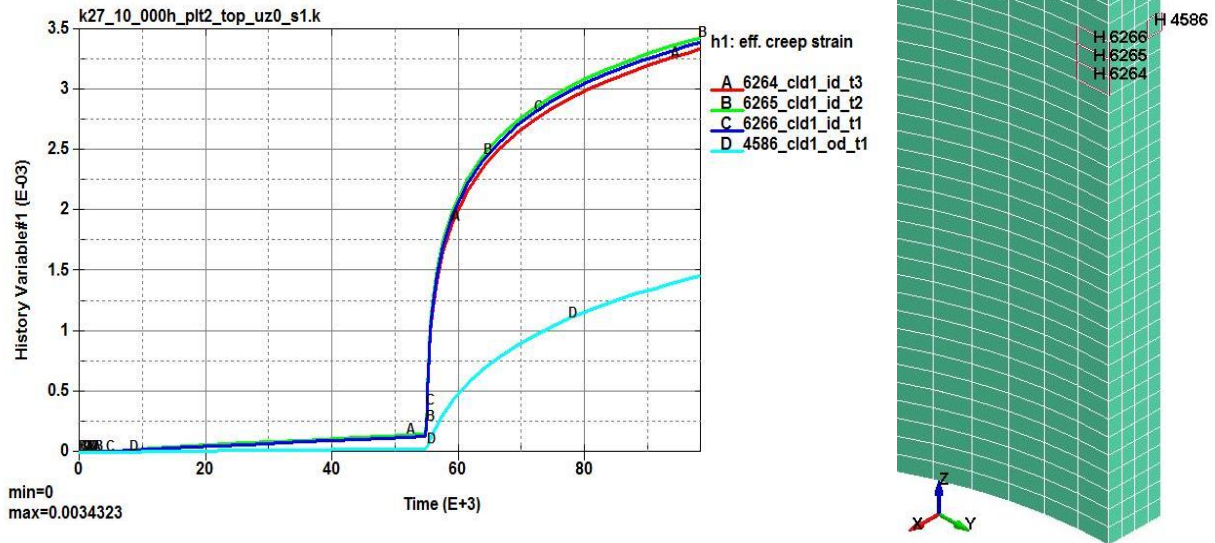


Figure 10: Effective creep strain versus time at mid height of the clad.

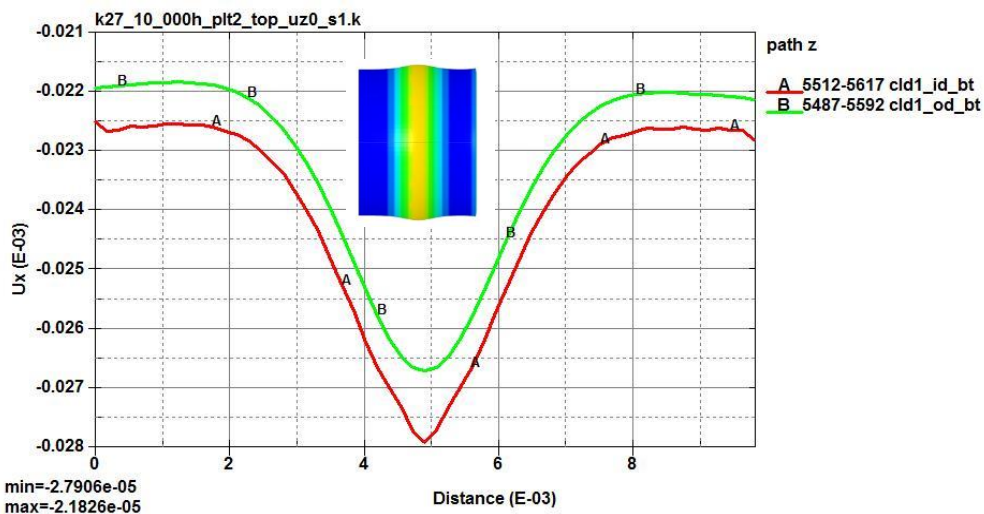


Figure 11: Clad radial displacement from bottom to top at the end of the ramp, meters.

The clad ridging behavior is shown in Figure 11 in the form of clad radial displacement from bottom to top at the end of the ramp. The insert shows the deformed shape that was magnified by 80X for visualization. The amount of ridging is defined as the difference in U_x on clad OD between bottom and mid height, ΔU_x . Thus $\Delta U_x = 4.79 \mu\text{m}$ in this case. Summarizing results for 600h and 1000h additional hold time; the conclusion is that the amount of ridging is not sensitive to the hold time at the 50% power, as can be inferred from Figure 10, which shows insignificant creep strain and small slope at the 50% power level.

3.4 Effect of Missing Pellet Surface

As shown in Figure 1, geometrical defects of missing pellet surface (MPS) can exacerbate PCMI and caused fuel rod failure. Simulations of MPS cases can determine the effects of various sizes of MPS on clad hoop stresses, and provide guidance on quality control of inspections, and useful for PCMI failure risk assessment. The model in Figure 12 shows an example with a large MPS.

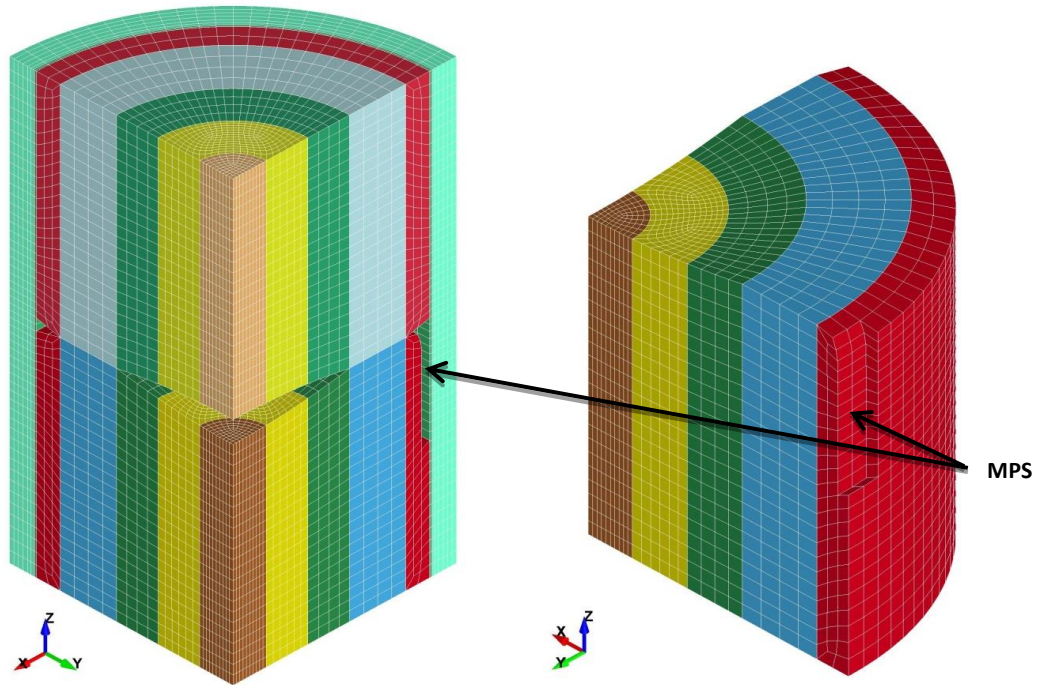


Figure 12: Example of model with a large MPS.

The temperature and the 1st principal stress contours in clad for this case is shown in Figure 13. It is evident that the MPS significantly increased the stresses in the clad, and reduced the local temperature.

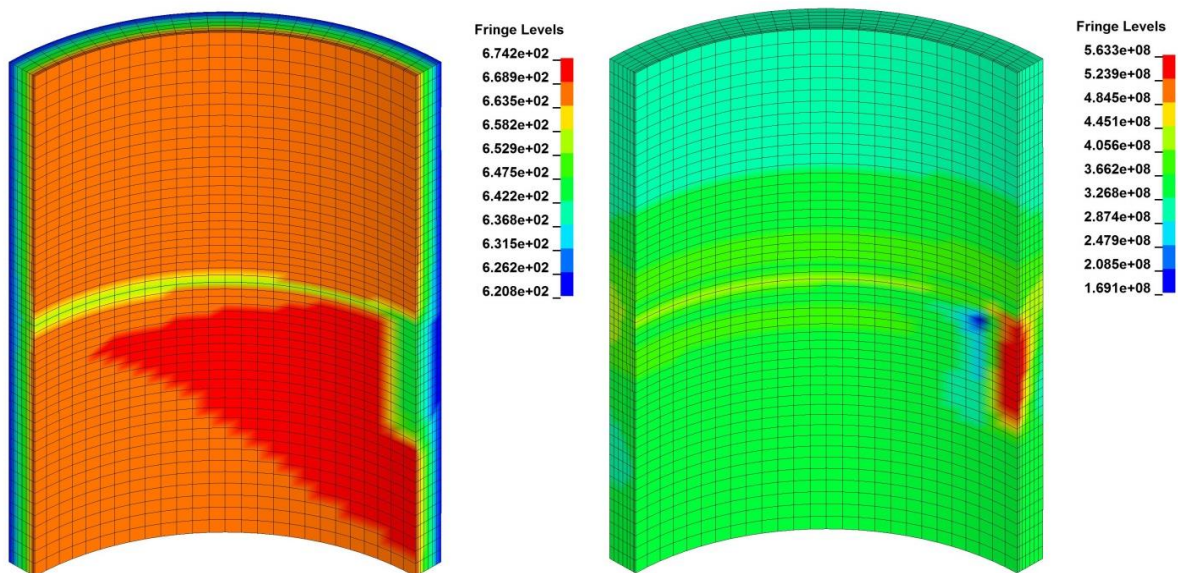


Figure 13: Temperature (left) and the 1st principal stress (right) contours in clad.

The effect of MPS sizes on clad hoop stress is plotted in Figure 14 for a few smaller MPS sizes, where “mps 0” is the reference case of without MPS; “mps a1c3” denotes MPS size that is 1 element in the axial direction, and 3 elements in the circumferential direction, and so on. The distance is measured from the clad ID to OD at the mid height of the model.

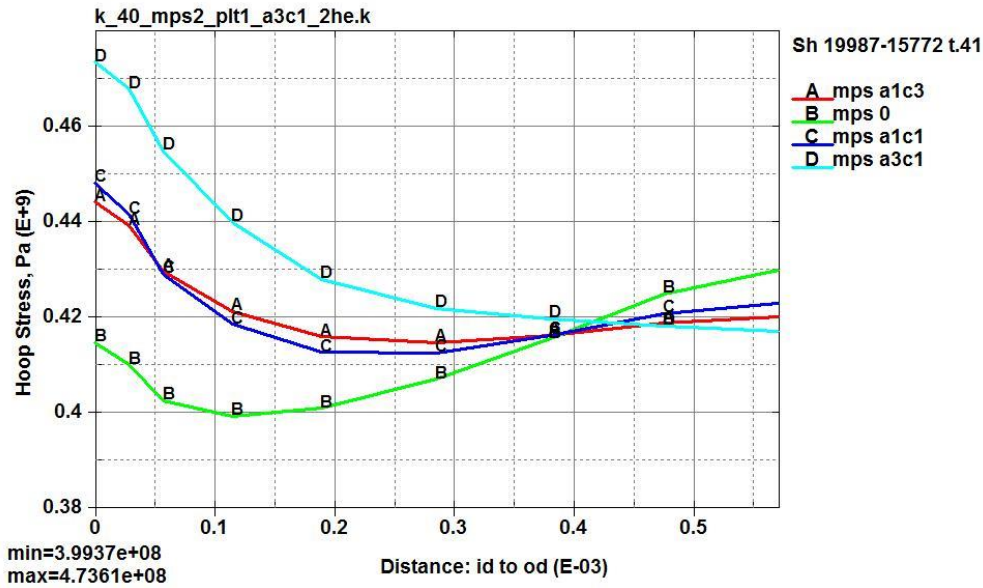


Figure 14: effect of MPS sizes on clad hoop stress.

3.5 Effect of Pellet Crack

As a brittle material subjected to high thermal stresses, pellet cracks in radial, circumferential (e.g. Figure 1) and axial directions. The cracking behavior is further complicated by the random nature of its microstructure and the fission products release and accumulation at the grain boundaries. Towards initial understanding of pellet crack on clad stress concentration, a potential radial crack at a pre-specified location in the lower pellet, Figure 15, is considered. The radial crack is considered as it has the most significant stress concentration effect on clad.

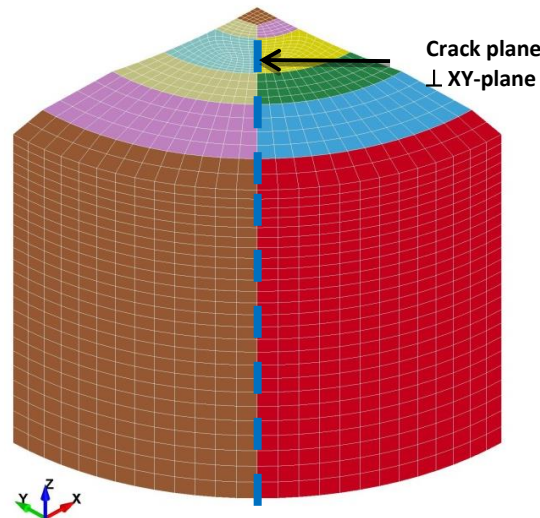


Figure 15: Potential radial crack in the lower pellet.

The crack plane, Figure 15, is modeled as a contact interface with failure behavior controlled by the interface bonding strength in normal and tangential directions, such that the contact surfaces separate when the strength is exceeded.

Snap shots of crack progression are shown in Figure 16 for the power ramp scheme shown in Figure 8. The color contour represents the temperature. The displacements are magnified by 25x to show crack opening. It can be seen that no cracking occurred at 50% power. Pellet cracked during power ramp from 50% to 100%. The further opening of the crack after holding at 100% power is attributed to reduced constraint from clad due to cladding creep.

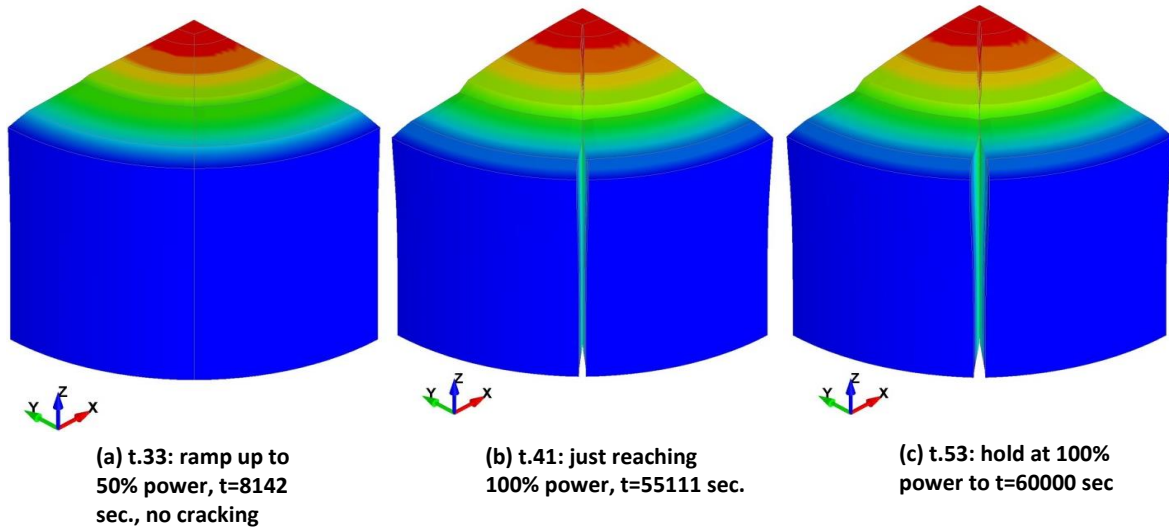


Figure 16: Snap shots of pellet crack progression during power ramp.

The hoop stress distribution in clad along the ID of circumference at mid height is shown in Figure 17 for three different times corresponding to those in Figure 16. It is evident of the stress concentration caused by cracking, and the effect of cladding creep.

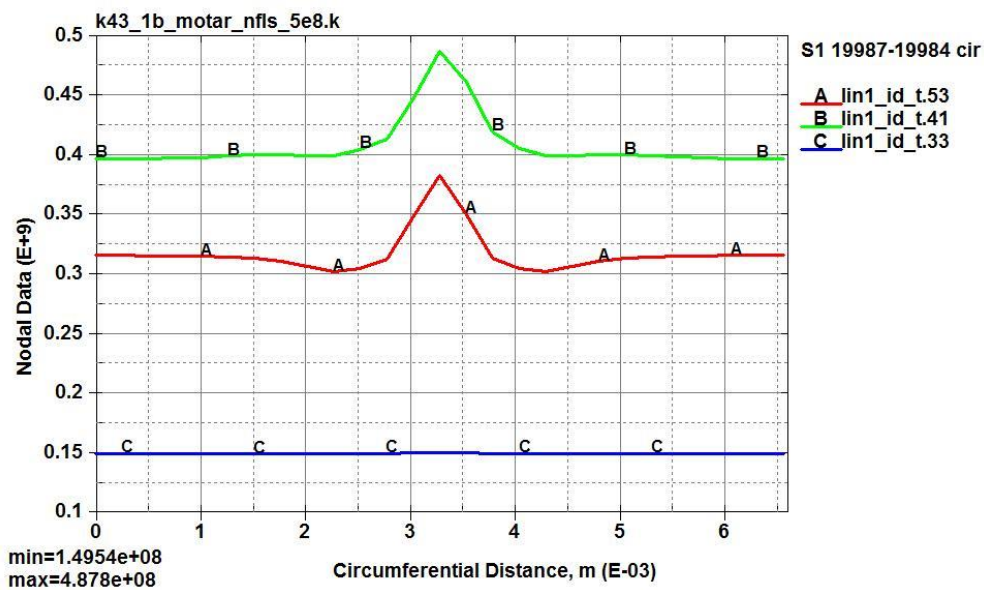


Figure 17: Clad hoop stress distribution along the ID of circumference at mid height.

4. Concluding Remarks

A coupled thermal-structural LS-DYNA model suitable for simulating the complicated PCMI phenomena under steady-state operations, operational transients, and accident conditions has been developed. The capability of the model has been demonstrated using various application examples presented, including off-centered pellet, missing pellet surface, and pellet cracking. The model will be extended, enhanced, and used to help understand the PCMI behavior and provide guidance to design, fabrication and operations.

References

- [1] W. Zhao, J. Liu, W. Stilwell, B. Hempy, and Z. Karoutas, Modeling Nuclear Fuel Rod Drop with LS-DYNA®, 13th International LS-DYNA Users Conference, 2014.
- [2] P.J. Sipush and R.S. Kaiser, The Effect of Power Change on the PCI Failure Threshold, *Rex Mechanica* 15 (1985) 275-295. <http://www.iaea.org/inis/collection/NCLCollectionStore/Public/33/022/33022442.pdf>
- [3] Y. Aleshin, C. Beard, G. Mangham, D. Mitchell, E. Malek, M. Young, The Effect of Pellet and Local Power Variations on PCI Margin, Proceedings of Top Fuel 2010, Sept. 26-29, 2010, Orlando, Florida, USA, Paper 041.
- [4] W. A. Boyd, G. Mangham, A Westinghouse Local Fuel Duty PCI Risk Monitor and Analysis Tool, Proceedings of Top Fuel 2015, Sept. 13-17, 2015, Zurich, Switzerland, Paper A0206.
- [5] Beard, et al., Westinghouse Control Rod Ejection Accident Analysis Methodology Using Multi-Dimensional Kinetics, WCAP-15807-NP-A, Westinghouse Electric Company, LLC, 2003.
- [6] Foster, Sidener, and Slagle, Westinghouse Improved Performance Analysis and Design Model (PAD 4.0), WCAP-15063-NP-A, Rev. 1, Westinghouse Electric Company, LLC, July 2000.